

Proceedings of the Korean Nuclear Autumn Meeting
Yongpyong, Korea, October 2002

Comparison of Void Fraction Profiles in Subcooled Boiling of Low Pressure by 3D Measurement and MARS Calculation

Moon-Oh Kim, Seong-Jin Kim, and Goon-Cherl Park
Department of Nuclear Engineering, Seoul National University
San 56-1 Shinlim-Dong, Gwanak-Gu, Seoul 151-742, Korea
E-mail address: bluewon@gong.snu.ac.kr

Abstracts

The radial and axial characteristics of void fraction were measured in vertical concentric annulus for the subcooled boiling flow by two-conductivity probe. Experiments were carried at different levels of heat flux, mass flux, subcooling. The exit pressure of system is near the atmosphere. The range of average void fraction was up to 18% and that of the average liquid velocity were less than 0.85 m/sec. And area average void fractions measured at $L/D_h=90.5, 80.1, 71.4$ were compared with the calculation of MARS. Some subcooled boiling models were evaluated.

Keyword : void fraction, low pressure, subcooled boiling, RELAP

1. Introduction

Recently, the interest in the research reactor operated at low pressure has been increased. But it has been reported that RELAP, the general code for nuclear safety analysis, is poor at prediction in low pressure where the behavior of vapor is very sensitive to thermal non-equilibrium and flow conditions (Zeitoun & Shoukri, 1997). It is considered as the reason that the existing subcooled boiling correlations of RELAP are developed for high-pressure conditions.

Thus, the works to evaluate the subcooled boiling model have been actively

performed and the need to develop the subcooled boiling models which are applicable for low pressure conditions is stressed. Although many experimental data are required for models development, the experimental studies at low pressure are very lacked and even most of them were measured by averaging measurement methods using such as g -densitometer along axial direction (Rogers, 1987, Edleman, 1981), or experiments were conducted in air/water flow (Hibiki & Ishii, 2000, Euh, 2001).

However, the local measurement experiments of two-phase flow parameters along radial and axial direction are essential to develop more accurate subcooled boiling models and investigate the interaction mechanism between constitutive models. The local measurement of two-phase flow parameters makes it possible to evaluate individual variables consisting of constitutive models fundamentally, some of which are difficult to be measured accurately by averaging methods using gamma densitometer, and subcooled boiling models. In spite of its importance, local measurement is not found at all.

In this study, we gain research data for improvement of subcooled boiling models by 3D-measurement with axial and radial direction for two-phase flow parameters. Using a two-conductivity probe, the local values of void fraction were measured at 13 radial points in each 3 axial planes of the channel. Based on these experiment data, subcooled boiling models in MARS were evaluated.

2. Experiment

The schematic of the test loop is presented in Fig. 1. The test channel is a vertical concentric annulus of 2,870 mm long with a heated inner tube. The inner tube of 19 mm outer diameter is composed of a heated section and copper electrodes silver soldered to both ends of the heated section. The heated section is an 1,840 mm long inconel 625 tube with 1.5 mm wall thickness. The tube is uniformly heated by a 54 kW DC power supply. The outer tube is comprised of Pyrex tubes with 40 mm inner diameter, so that visual observation or taking photograph is possible.

Experiments were carried out at different levels of mass flux, heat flux and subcooling under the subcooled boiling. The tested range of the parameters was 317 ~ 681 kg/m²s for mass flux, 135 ~ 358 kW/m² for heat flux and 10.2-21.7 for subcooling. The inlet flow rate was regulated by flow control valve, and the inlet

temperature was controlled by the preheater. Also, the heat flux was controlled by the DC power supply. The water temperatures at the test channel inlet and exit were measured using the calibrated platinum resistance temperature detectors within ± 0.2 °C, and the pressures at inlet and measuring plane were measured by absolute pressure transducers with the estimated error of ± 0.001 MPa. The errors in mass flux, inlet temperature and heat flux measurements were estimated to be within ± 1.7 %, ± 2.2 % and ± 1.7 % of the rated values, respectively. The system pressure was maintained at 1 to 2 bar, and was not controlled but determined by net volume expansion balanced by the bubble generation rate in the test channel and the ventilation rate in the storage tank.

The two-conductivity probes were installed at three positions of $L/D_h=90.5$, 80.1 , 71.4 . The local void fraction was measured by a two-conductivity probe method (Lee and Park, 2001). The conductivity probe method is based on the use of the difference of electrical resistance between vapor and liquid phases. Two sensing element of two conductivity probe are made of teflon-coated stainless steel wires with a diameter of 0.076 mm and their tips are sharpened to a conical shape for minimizing the deformation of bubbles on impact with the probe. Each sensing wire is inserted into a 0.4 mm stainless steel tube, and fixed by a high temperature epoxy. Then the two sensors are inserted into a 1.6 mm stainless steel tube, and aligned in the axial direction of channel.

The change of resistivity sensed by each sensor was converted into voltage drop by an A.C. rectifier circuit. Generally, the voltage signals deviate from the ideal two-state square-wave signals mainly due to the finite size of the sensor and the possible deformation of the vapor bubble interface before the sensor enters from one phase to the other. Thus, the proper threshold voltage indicating the boundary between the two phases has to be used as a phase discrimination criterion. In this study, the threshold voltage is calculated based on the pulse height and slope criterion for each bubble. The threshold voltage for each bubble is assumed to be proportional to the pulse height produced by an individual bubble, and is calculated as follows.

$$H_T = S (H_G - H_L) + H_L \quad (1)$$

In Eq. (1), H_T is the threshold voltage, S is the proportional constant, and H_G and H_L are the voltage levels by vapor and liquid phases, respectively. Even though a pulse is treated as a bubble by the threshold voltage, multi-peaked signals above the threshold voltage can exist, which can be caused by multi-bubble contact or wetting of

the probe tips. These bubbles are discriminated as separate bubbles by the slopes of the signals. Main advantage of the present algorithm is that the threshold voltage for each bubble is varied in accordance with the signal drift induced by probe fouling, change of flow condition and water conductivity.

The proportional constant was pre-determined by air-water experiments in the transparent tube with two quick closing valves. The local void fractions were measured by using the proportional constants of 0.1~0.9, and then area-averaged values were compared with the void fraction by the quick closing valve technique. From the comparison, the optimum proportional constant was determined to be 0.35. The local void fraction was determined by dividing the accumulated time that the probe sensor was exposed to the vapor phase by the total sampling time. The total sampling time should be sufficiently long enough for statistical treatment. The local void fraction was found to be nearly constant after about 20 seconds of integration time. In the present experiments, total sampling time for each local position was set to be 1 minute, which is long enough to satisfy the repeatability of void fraction. Also, The uncertainty associated with local void fraction measurement was estimated to be $\pm 3\%$.

3. Experiment Results

The axial and radial profiles of local void fraction are shown in Fig. 2. The void fraction is one of fundamental parameters that characterize the structure of boiling flow because it reflects the energy of fluid and influences the distributions of other local parameters. In those figures, $(r-R_{inner})/(R_{outer}-R_{inner})=1$ indicates the inner surface of the outer tube wall, and $(r-R_{inner})/(R_{outer}-R_{inner})=0$ means the heated surface. In the present experiments, the void fraction at the position less than 0.11 of $(r-R_{inner})/(R_{outer}-R_{inner})$ were not measured due to the probe geometry.

The local void fraction decreases from the heated surface to the subcooled liquid core and from higher measuring section to lower measuring section. The peak local void fraction is almost observed near the heated surface, and its value increases with the wall heat flux and axial position. But it is found that the position of the peak of local void fraction in higher void fraction moves toward to center of flow channel for large vapor size due to coalescence of vapor and increased enthalpy of subcooled liquid. If the void fraction increases about to 17%-20%, the size of vapor becomes 4–6 mm and this fact

implies that the flow pattern changes to slug flow with high void fraction.

Fig. 2 shows the thickness of bubble boundary layer increases with the wall heat flux and axial position, and decreases with mass flux and subcooling. The existence of two distinguishable flow regions in the flow channel is made by the thermal non-equilibrium of two phases. One of the regions is the bubble boundary layer as the two-phase region adjacent to a heated surface and the other is the subcooled liquid core. The bubble boundary layer of higher measuring position is thicker than that of low measuring position along axial direction with heated surface by process of bubble coalescence and volume expansion due to the increase of bubble generation and enthalpy as moving along heated surface. Fig. 3 shows the increasing bubble layer along heated surface above described by photographic. These photographs were pictured at a speed of 1000 frame/s using high-speed video camera.

4. Comparison of Measured and Calculated Void Fractions by MARS

In this study, interfacial heat transfer coefficient models and wall vapor generation models which play an important role in subcooled boiling flow are evaluated in the calculation of MARS (Multi-dimensional Analysis of Reactor Safety) based on RELAP5/MOD3, as summarized in Table 1. It is being developed by KAERI (Korea Atomic Energy Research Institute) for the multi-dimensional and multi-purpose realistic thermal-hydraulic system analysis of light water reactor transients.

The first evaluation of subcooled boiling model has a relation with the interfacial heat transfer coefficient model. MARS adopts Unal and Lahey model as default model. Interfacial heat transfer coefficient of Unal and Lahey decreases with void fraction faster than that of Unal due to smoothing factor which connects Unal model and Lahey model. In subcooled boiling flow, the decrease of interfacial heat transfer coefficient means that of condensation, which consequently results in the increase of void fraction. Considering this effect, interfacial heat transfer model without smoothing factor and multiplier factor 0.075 as shown Table 2, Unal model, was implemented. This removing can be justified because all cases of this experiment have average void fraction less than 0.25. However, the rapid increase of void fraction in the region larger than 0.25 for the calculation is inevitable.

The second evaluation is related to the wall vapor generation model.

Saha-Zuber-Lahey model and SRL model (C. G. Thurston, 1992) is evaluated each in MARS 2.0 and MARS 2.1. The original MARS 2.0 adopts the critical enthalpy of Saha-Zuber-Lahey as shown Table 2. The critical enthalpy, h_{cr} , is corresponding to the bubble departure point.

When the liquid enthalpy is greater than the critical enthalpy, the heat flux fraction causing evaporation is $Frac_{s-z}$ of Table 2, which is the fraction of the wall heat flux used for evaporation increases from zero at the OSV point to one when the bulk liquid enthalpy reaches the saturation enthalpy. The pumping factor in the denominator of Table 2 is defined as the ratio of the pumping to the evaporation component of the wall heat flux. The original MARS 2.1 replaced critical liquid enthalpy and the evaporation fraction of Saha-Zuber by SRL model as shown in Table 2.

Run No. BC2 and BC13 of Zeitoun (1994) were used to examine the validity of MARS calculations. Zeitoun's experiment result and MARS calculation results were compared in Fig. 4. MARS 2.0 considerably under-predicted void fraction data of Zeitoun, but MARS 2.1 and modified MARS 2.1 agree with the experiment data.

But these situations are reversed in comparison of SNU experiments and MARS calculations. As shown in Fig. 5-6, SNU experiments agree with MARS 2.0 rather than MARS 2.1. Both MARS 2.1 and modified 2.1, all of which adopt SRL model in wall vapor generation model, over-predicts largely void fraction than MARS 2.0, and modified 2.1 slightly under-predicts experiment results than original 2.1. The one reason for over-prediction in MARS 2.1 is inferred from the way SRL model calculates critical heat flux smaller than Saha-Zuber-Lahey model. This causes OSV point and pumping factor e suppression of the evaporation process to be lower.

The difference original MARS 2.1 and modified MARS 2.1 is on different interfacial heat transfer coefficient model. Therefore, it could be concluded that wall vapor generation model is more dominant for prediction of void fraction than the interfacial heat transfer coefficient model in subcooled boiling flow.

Fig. 7 shows the comparison of measured data and predicted void fraction. MARS 2.0 agrees with experiment data within the average deviation of $\pm 35\%$ but MARS 2.1 and modified MARS 2.1 largely over-predicts than experiment data.

Conclusion

(1) The radial and axial characteristics of local void fraction were experimentally investigated in vertical concentric annulus for the subcooled boiling flow.

(2) Measurements showed that the local void fraction decreases from the heated surface to the subcooled liquid core and from higher measuring section to lower measuring section.

(3) The peak local void fraction is almost observed near the heated surface. But it is found that the position of the peak of local void fraction in higher void fraction moves toward to center of flow channel for large vapor size

(4) MARS 2.0 under-predicts void fraction than McMaster calculation, but agrees with this experiment.

(5) In the subcooled boiling region, the effect of wall vapor generation model modification is larger than that of interfacial heat transfer model in prediction of void fraction. Additional evaluating of subcooled boiling model is required in low pressure

Nomenclature

ρ_f	density of the liquid phase
ρ_g	density of the gas phase
h_f	enthalpy of the liquid phase
$h_{f,sat}$	saturation enthalpy of the liquid phase
h_{fg}	latent heat of vaporization
C_{pf}	specific heat capacity of the liquid phase
Q_{evap}	vapor formation heat flux
Q_{pump}	pumping heat flux
St	Stanton Number
Nu	Nusselt Number

References

AEA Technology, 1998, User's Manual to CFX Version 4.2, AEA Technology plc, Harwell, UK.

Anglart, H. and Nylund, O., "CFD Application to Prediction of Void Distribution in Two-Phase Bubbly Flows in Rod Bundles," Nuclear Engineering and Design, Vol. 163, pp.81, 1996.

Bibeau, E.L. and Salcudean, M., "Subcooled Void Growth Mechanisms and Prediction at Low Pressure and Low Velocity," Int. J. Multiphase Flow, Vol. 20, No. 5, pp. 837-863, 1994.

C. G. Thurston, "RELAP5/MOD3 Benchmarks of Low Pressure Subcooled Vapor Voiding in Annular Flow Channels," Babcock & Wilcox Advanced Systems Engineering, Doc. 51-3001526-00, July 1992.

DelValle, J.M. and Kenning, D.B.R., "Subcooled Flow Boiling at High Heat Flux," Int. J. Heat and Mass Transfer, Vol. 28, pp. 1907-1920, 1985.

Dix, G.E., "Vapor Void Fraction for Forced Convection With Subcooled Boiling at Low Flow Rate," General Electric Report NEDO-10491, 1970.

Edleman, Z. and Elias, E., "Void Fraction Distribution in Low Flow Rate Subcooled Boiling," Heat Transfer Division, ASME, Winter Annual Meeting.

Euh, D.J., A study on the Measurement Method and Mechanistic Prediction Model for the Interfacial Area Concentration, Ph.D. Thesis, Seoul National University, Korea, 1996.

Griffith, P., Clark, J. A. and Rohsenow, W. M., "Void Volumes in Subcooled Boiling," ASME Paper 58-HT-19, U.S. National Heat Transfer Conf., Chicago.

Hibiki, T. and Ishii, M., "One-Group Interfacial Area Transport of Bubbly Flows in Vertical Round Tubes," Int. J. Heat and Mass Transfer, Vol.43, pp. 2711- 2726, 2000.

Ishii, M. and Zuber, N., "Drag Coefficient and Relative Velocity in Bubbly, Droplet or Particulate Flows," AIChE Journal, Vol. 25, No. 5, pp. 843-855, 1979.

Ishii, M. and Mishima, K., "Study of Two-Fluid Model and Interfacial Area," NUREG/CR1873, 1980.

Ishii, M. and Revankar, S.T., "Measurement of Interfacial Area Using Four Sensor Probe in Two Phase Flow," DOE/ER/14147, July, 1991.

Kataoka, I., Ishii, M. and Serizawa, A., "Local Formulation and Measurements of

Interfacial Area Concentration in Two-Phase Flow," Int. J. Multiphase Flow, Vol.12, NO.4, pp. 505-529,1986

Lee,T.H. and Park,G.C., "Experimental Investigation on Drift Flux Parameters for Subcooled Boiling in a Vertical Annulus," Int. Comm. Heat Mass Transfer, Vol.28, No.2, pp.191-200, 2001.

Neal, L.G. and Bankoff, S.G., "A High Resolution Resistivity Probe for Void Fraction Measurements in Air-Water Flow," AIChE J. pp. 490-494, 1963.

Rogers, J.T., Salcudean, M., Abdullah, Z., McLeod, D. and Poirier, D. "The Onset of Significant Void in up-Flow Boiling of Water at Low Pressure and Low Velocities, " Int.J. Heat Mass Transfer, Vol. 30, No. 11, pp. 2247-2260,1987.

RELAP5/MOD 3.3.2 Code Manual, NUREG/ CR- 5535, INEL-95 / 0174,Vol.1

Rouhani, S.Z. and Axelsson, E., "Calculation of Void Volume Fraction in the Subcooled and Quality Boiling Region, " International Journal of Heat and Mass Transfer, Vol. 13, pp. 383-393, 1970.

Tu, J.Y., Yeoh, G.H., "On numerical modeling of low pressure subcooled boiling flows," Vol.45, pp. 1197-1209, 2002.

Unal, H.C., "Maximum Bubble Diameter, Maximum Bubble Growth Time and Bubble Growth Rate During the Subcooled Nucleate Flow Boiling of Water up to 17.7MN/m², " Int. J. Heat and Mass Transfer, Vol. 19, pp. 643-649, 1976.

Yun, B.J., Song, C.H., Sim, S.K., Chung, M. K. and Park, G.C., "Measurements of Local Two-Phase Flow Parameters in a Boiling Flow Channel," OECD/CSNI Special Meeting on Advanced Instrumentation and Measurement Techniques, Santa Barbara, 1997.

Zeitoun, O, Subcooled Flow Boiling and Condensation, Ph.D Thesis, McMASTER University, Canada, 1994.

Zeitoun, O. and Shoukri, M., "Axial Void Profile in Low Pressure Subcooled Flow Boiling," Int. J. Heat and Mass Transfer, Vol. 40, No. 4, pp. 869-879, 1997.

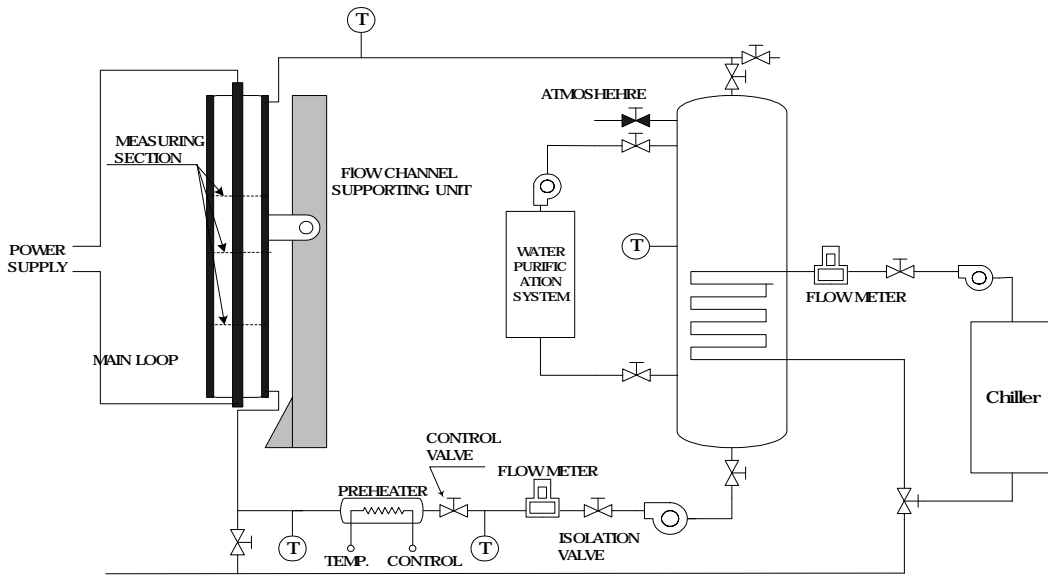


Fig. 1 Schematics of experiment facility

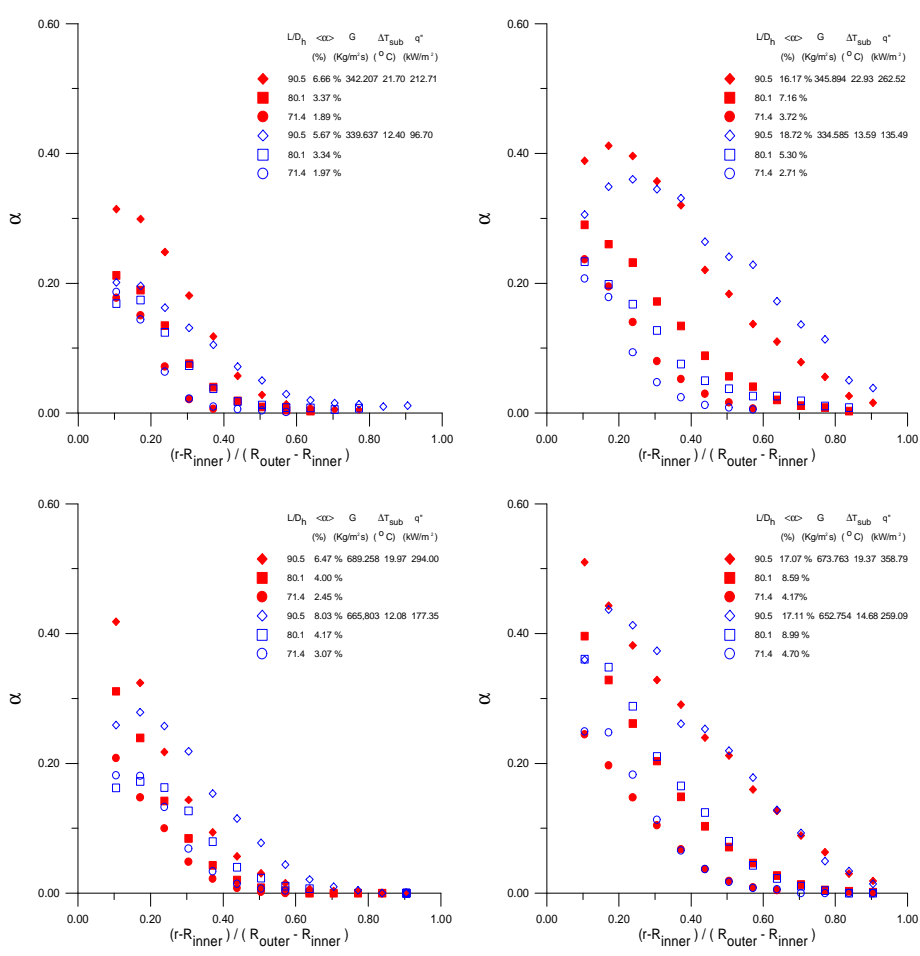


Fig. 2 Axial and Radial distribution of Void Fraction

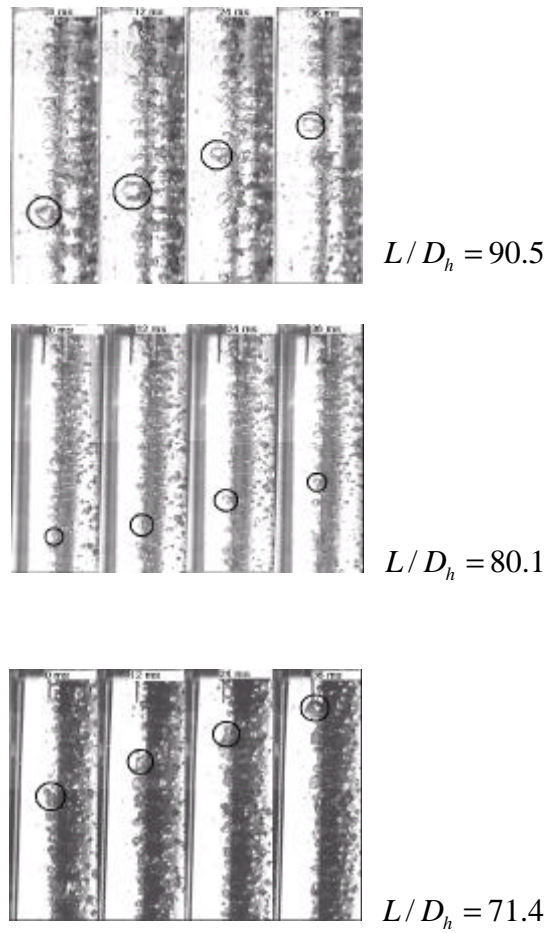


Fig. 3 Photography of vapor layer along axial direction

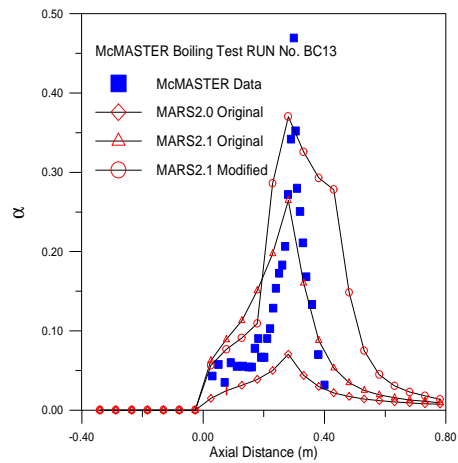


Fig. 4 Comparison of McMaster's experiments and calculation by MARS

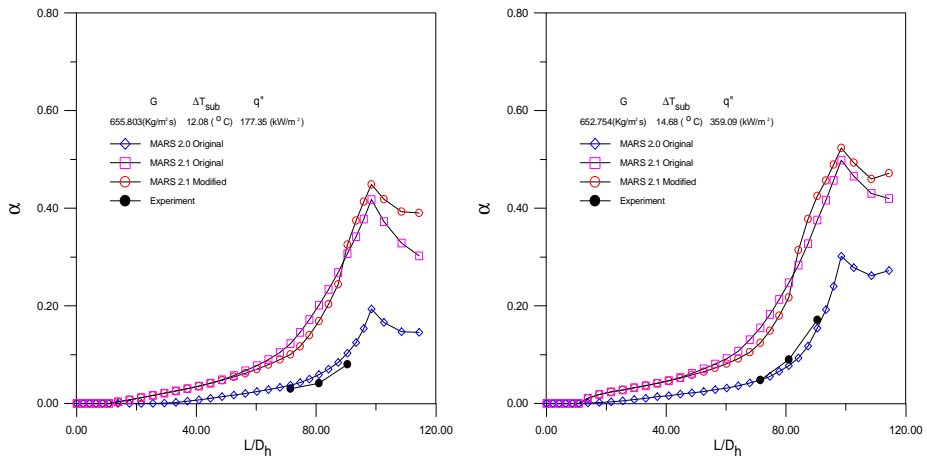
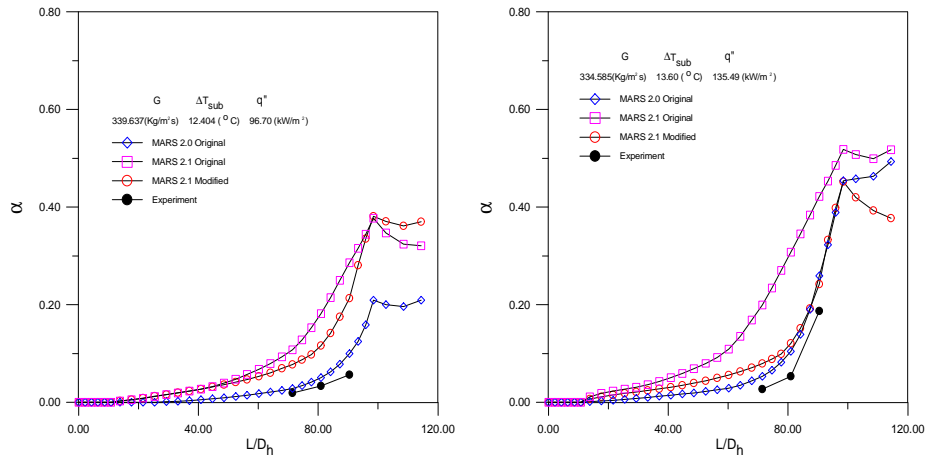
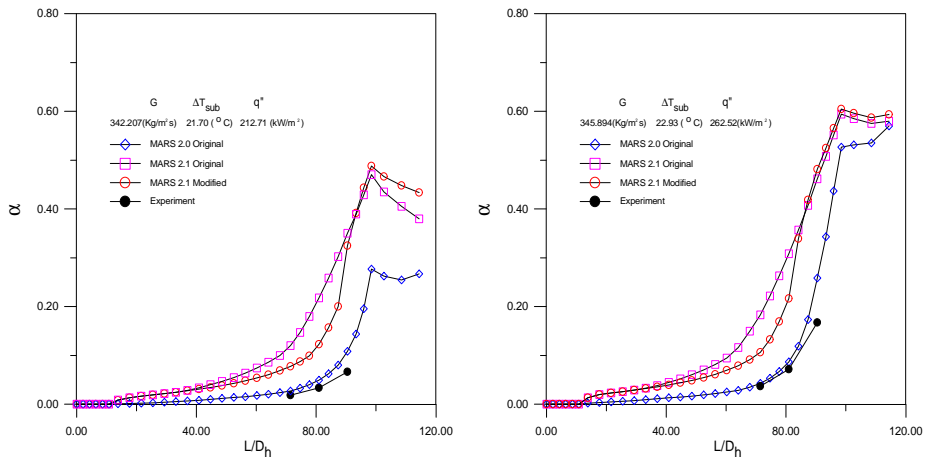


Fig. 5 Comparison of measured and calculated by MARS-high subcooling



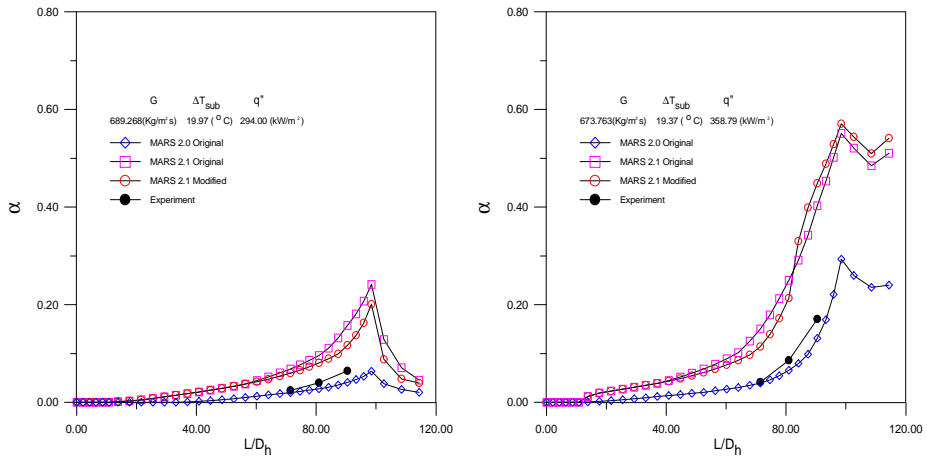


Fig.6 Comparison of measured and calculated by MARS-low subcooling

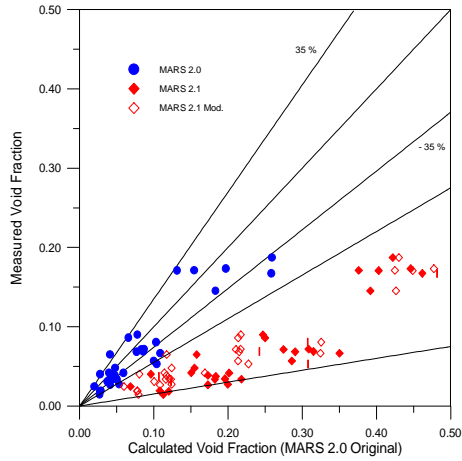


Fig. 7 Comparison of measured and calculated void fraction

Table 1.Evaluation Table

	MARS 2.0	MARS 2.1	MARS 2.1 modified
Interfacial Heat Transfer Coefficient	Unal and Lahey	Unal and Lahey	Unal
Wall Vapor Generation Model	Saha-Zuber and Lahey	SRL	SRL

Table 2 Subcooled boiling models in MARS

<p>Interfacial Heat Transfer Model -Unal and Lahey</p>	$h_{if} = \begin{cases} [0.075 + 1.8 \cdot C \cdot \Phi \cdot \exp(-45 \cdot a)] \cdot \frac{h_{fg} r_{vap} r_{liq} D_{bub}}{2(r_{liq} - r_{vap})} & a_{bub} < 0.25 \\ 0.075 \cdot \frac{h_{fg} r_{vap} r_{liq} D_{bub}}{2(r_{liq} - r_{vap})} & a_{bub} > 0.25 \end{cases}$ $C = 65.0 - 5.69 \times 10^{-5} (P - 1.0 \times 10^5) \quad P \leq 1.1272 \times 10^6 \text{ pa}$ $\Phi = \begin{cases} 1 & v_f \leq 0.61 \text{ m/s} \\ (1.639344 v_f)^{0.47} & v_f > 0.61 \text{ m/s} \end{cases}$
<p>Wall Vapor Generation Model Saha-Zuber Model</p>	$h_{cr} = \begin{cases} h_f^s - St \frac{C_{pf}}{0.0065} & (\text{for } Pe > 70,000) \\ h_f^s - Nu \frac{C_{pf}}{455} & (\text{for } Pe \leq 70,000) \end{cases}$ $Frac_{S-Z} = \frac{h_f - h_{cr}}{(h_f^s - h_{cr})(1 + e)}$ $e = \frac{Q_{pump}}{Q_{evap}} = \frac{r_f (h_f^s - h_{cr})}{r_g h_{fg}}$
<p>Wall Vapor Generation Model SRL model</p>	$h_{cr} = h_f^s - \frac{St \times C_{pf}}{(0.0055 - 0.0009 * fprgmm)}$ $fprgmm = 1.0782 / (1.015 + \exp(p / psia - 140.75) / 28.0)$ $psia = 6.894757e3, \text{ units conversion}$ $Frac_{SRL} = gmmlp / (1.0 + r_f \times (h_f^s - h_f) \times fpreps / (r_g \times h_{fg}))$ $gmmlp = crenhr + fprgmm \times (p5r - crenhr)$ $crenhr = (h_f - h_{cr}) / (h_f^s - h_{cr})$ $fpreps = 1.0 / (0.97 + 38.0 \times \exp(-(pbr + 60.0) / 42.0))$ $fpreps = \min(1.0, fpreps)$ $fprgmm = 1.0782 / (1.015 + \exp((pbr - 140.75) / 28.0))$ $p5r = 0.0022 + crenht \times (0.11262 + crenhr \times (-0.59224 + crenhr \times (8.68227 + crenhr \times (-11.29044 + crenhr \times (4.253448))))))$ $p5r = \min(1.0, p5r)$